CHINESE OPTICS LETTERS

Vol. 22, No. 4 | April 2024

Neural network equalization based on delta-sigma modulation

Bo Liu (刘 博)[1*], Jianxin Ren (任建新)[1], Xiangyu Wu (吴翔宇)[1], Shuaidong Chen (陈帅东)[1], Yaya Mao (毛雅亚)[1], and Li Zhao (赵 利)[2]

[1] Nanjing University of Information Science & Technology, Nanjing 210044, China

[2] Key Laboratory for Information Science of Electromagnetic Waves (MoE), Fudan University, Shanghai 200433, China

*Corresponding author: bo@nuist.edu.cn

Received June 16, 2023 | Accepted January 11, 2024 | Posted Online April 26, 2024

We propose a neural network equalization delta-sigma modulation (DSM) technique. After performing DSM on the multi-order quadrature amplitude modulation (QAM) orthogonal frequency division multiplexing (OFDM) signal at the transmitting end, neural network equalizer technology is used in the digital signal processing at receiving end. Applying this technology to a 4.6 km W-band millimeter wave system, it is possible to achieve a 1 Gbaud 8192-QAM OFDM signal transmission. The data rate reached 23.4 Gbit/s with the bit error rate at 3.8×10^{-2}, lower than soft-decision forward-error correction threshold (4×10^{-2}).

Keywords: multi-order quadrature amplitude modulation; W-band; delta-sigma modulation; neural network equalization; nonlinear compensation.

DOI: 10.3788/COL202422.040601

1. Introduction

The potential of millimeter wave (MMW) communication systems as a promising solution for future broadband wireless access is widely acknowledged, given their ability to support multi-Gbit/s services easily. Consequently, they are regarded as a strong candidate for inclusion in upcoming 5G and ultra-5G wireless networks. MMW technology provides better directionality and wider bandwidth than traditional microwave wireless systems, as evidenced by comparative analysis. MMW communication systems have been the subject of numerous studies and experimental demonstrations of their application in 5G technology, as documented in the literature[1–4], especially, W-band (75–110 GHz), which is a high-frequency band allocated for various applications including wireless communication, radar, and imaging systems.

Despite recent advancements in technology, the limited bandwidth of electronic devices remains a bottleneck for further increasing capacity. To tackle this challenge and enable multi-Gbit/s MMW transmission, researchers have explored photonics-assisted MMW technology with high-order quadrature amplitude modulation (QAM) and generation[5–11]. Higher-order QAM signal transmission requires higher signal-to-noise ratios (SNRs) and higher digital-to-analog converter (DAC) resolution. Recently, in research based on network feedforward, ultrahigh order QAM transmission has been achieved by replacing the traditional common public radio interface (CPRI) with delta-sigma modulation (DSM) technology, improving spectral efficiency[12–16]. DSM technology can convert high-order QAM signals to 1-bit signals for transmission, alleviating some of the problems caused by ultrahigh-order QAM transmission[13–15]. The 1-bit quantized signals in QAM transmission are equivalent to quadrature phase shift keying (QPSK) signals, providing a higher SNR tolerance. However, when the wireless transmission distance is too long, it can decrease the system SNR and system nonlinearity, including nonlinearity from wireless channels and photoelectric devices, such as optical modulators and electrical amplifiers (EAs). This, in turn, leads to contact between signal constellation points, affecting the correct judgment of the signal. Neural network equalizers (NNEs) that can accurately represent and correct nonlinear effects are a promising solution for nonlinear compensation (NLC)[17–21]. With data-aided training, NNEs can adaptively fit the signals' time-delay nonlinearity using multilayer weight-controlled accumulation of nonlinear activation functions, outperforming traditional Volterra-series-based NLC.

In this Letter, we experimentally demonstrate 8192-QAM orthogonal frequency division multiplexing (OFDM) signal transmission over a 4.6-km wireless distance at W-band, achieving a transmission rate of 1 Gbaud with the aid of DSM and NNE technologies. To our knowledge, this is the first time that 1 Gbaud 8192-QAM OFDM signal transmission has been demonstrated over such a distance.

2. Principle of DSM

First, offline MATLAB software generates pseudo-random binary sequences (PRBSs) and then converts them into higher-order QAM signals through QAM mapping. We use the Mersenne twister algorithm (MT-19937) for generating PRBS instead of traditional generation polynomial (e.g., PRBS-15). In this way, PRBS with much higher quality than traditional PRBS can be generated, which has a period of $2^{19937}-1$ (around 6.95×10^{59} numbers, a lot more than $2^{15}-1$ using PRBS-15), alleviating the overestimation problem caused by NN models. The fast Fourier transform (FFT) length is set to 1024, with the position of the first subcarrier of the OFDM signal at 0 for DC bias. Among the remaining 1023 subcarriers, 980 subcarrier signals are used to load multi-order QAM signals, and the remaining subcarriers are zeroed. We convert the signal in the frequency domain to the time domain, add a cyclic prefix with the length of 64 to the signal, and generate a frame of OFDM signal. A frame of OFDM signal consists of 100 OFDM signals, which are oversampled 10 times. The same 1-bit quantization is used for the real and imaginary parts of the OFDM signal in the time domain, and the QPSK signal is obtained for transmission. Before generating OOK signals, we need to generate a transfer function, which is generated by invocating the synthesizeChebyshevNTF function in MATLAB. Invocate the synthesizeChebyshevNTF function as follows: H = synthesizeChebyshevNTF (order, OSR, opt, H_inf, f_0). By running the above functions, we get the following transfer functions:

$$H=\frac{(z^2-1.993z+1)(z^2-1.95z+1)(z^2-1.909z+1)}{(z^2-1.594z+0.6419)(z^2-1.641z+0.7272)(z^2-1.758z+0.8918)}. \tag{1}$$

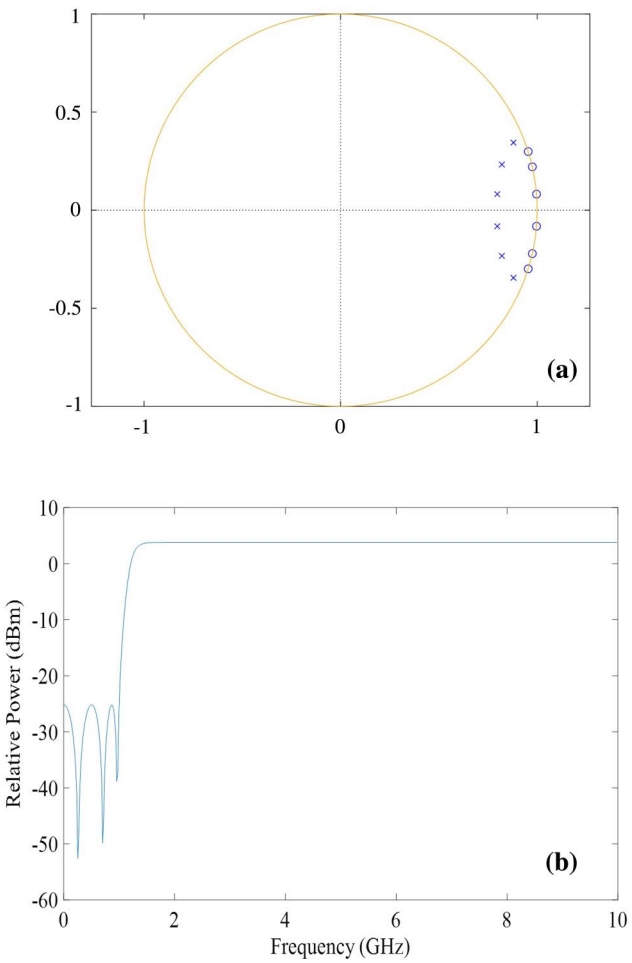

Fig. 1. Noise transfer function. (a) Zero points and pole points; (b) frequency response of amplitude.

Equation (1) shows the transfer function with an oversampling ratio of 10 and 1-bit quantization. Figures 1(a) and 1(b) show the zero points and pole points and the frequency response of amplitude of the noise transfer function, respectively.

In order to generate QPSK signals, we also need to invocate the simulateDSM in the DSM toolbox in MATLAB. We invocate the simulateDSM function and input the OFDM signal (u_1 + i·u_2) and transfer function H after oversampling. We run the following function: v_1 = simulateDSM (u_1, H), v_2 = simulateDSM (u_2, H). Then the QPSK signal v = complex (v_1, v_2) to be transmitted in the channel is obtained.

After capturing the signals by digital OSC at the receiver, we use offline digital signal processing (DSP) to recover the signals further. We use neural network-based equalization to compensate for the linear and nonlinear effects caused by the transmitter, receiver, and wireless channel. The structure of the proposed NNE is shown in Fig. 2.

$$X=\{x_1,x_2,\ldots,x_{2t}\},\qquad s_i=x_{2i-1}+x_{2i}\cdot 1j. \tag{2}$$

After normalization and I/Q separation, the signal in the window is then sent to the input layer of the neural network. The data are then passed into the hidden layers to realize nonlinear compensation. The hidden layers are different weighted matrices W_1 and W_2 sized $2t\times m$ and $t\times n$, respectively. Each of the hidden layers can be regarded as linear fitting, and the output can be written as

$$H_{\text{out}}=H_{\text{in}}\cdot W+b. \tag{3}$$

Here, b is the bias. The output of each hidden layer is nonlinearized using the nonlinear activation function, and the multilayer weight-controlled accumulation of nonlinear activation

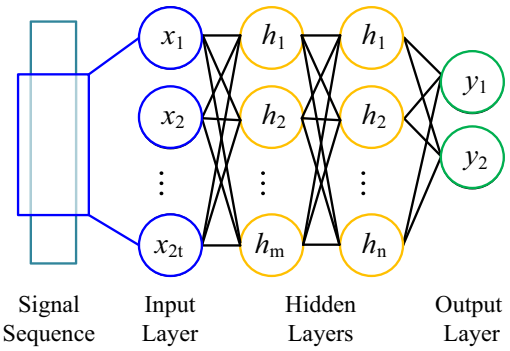

Fig. 2. Principle of NNEs.

functions makes NNE able to fit the nonlinear channel response. We used $\mathrm{ReLu}(\cdot) = \max(\cdot, 0)$ as the activation function.

Finally, the data are passed through the output layer, a weighted matrix W_3 shaped $n \times 2$. The output 2 neurons $\hat{Y} = [\hat{y}_1, \hat{y}_2]$ refer to the I/Q parts of the equalized signal. The whole forward propagation progress can be expressed as

$$Y = \mathrm{ReLu}(\mathrm{ReLu}(\mathrm{ReLu}(X \cdot W_1 + b_1) \cdot W_2 + b_2) \cdot W_3 + b_3. \tag{4}$$

To optimize the NNE's weights and biases, synced original signal Y is used to train the NNE. By using the mean square error (MSE) loss function as follows, the weights are optimized by backpropagation of the neural network:

$$\mathrm{MSE} = \sum (Y - \hat{Y})^2. \tag{5}$$

After neural network nonlinear compensation, the QPSK signal is restored, and then the high-order QAM OFDM signal in the time domain is restored through hard-decision, low-pass filtering. Finally, the OFDM signal in the time domain is converted into a QAM signal in the frequency domain, and the bit error rate (BER) of the signal is calculated.

The proposed NNE-based DSM scheme is essential to achieve the 1-Gbaud 8192-QAM transmission over 4.6 km wireless channel: DSM significantly increases tolerance for SNR and DAC precision. NNE can compensate for complicated nonlinearities caused by the channel and the transceivers, recover the DSM signals, and achieve BER below soft-decision forward-error correction (SD-FEC).

3. Experimental Setup

The experimental setup for W-band polarization multiplexing wireless transmission over a distance of 4.6 km, utilizing photonics-assisted technology, is depicted in Fig. 3. The Guanghua Building in the Handan campus, situated at an elevation of 142 m, serves as the transmitting-side (Tx-side), while the receiving-side (Rx-side) is located at the Physics Building in the Jiangwan campus, with an elevation of 24 m. Figures 3(a)–3(e) depict photographs of the Guanghua Building, transmission link, Physics Building, transmitter, and receiver, respectively. Figure 4 shows the offline DSP for transmitter and receiver.

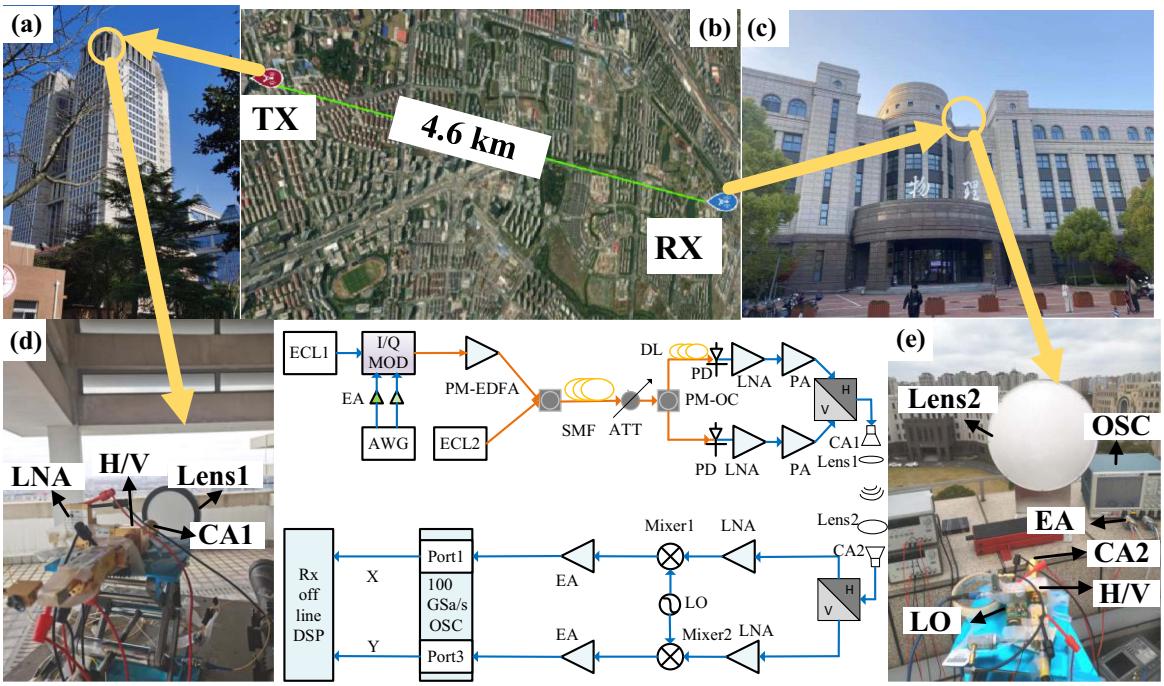

Fig. 3. Experimental setup of PDM-8192-QAM W-band wireless delivery over 4.6 km. Photos of (a) Guanghua Building in the Handan campus; (b) transmission link; (c) Physics Building in the Jiangwan campus; (d) transmitter; (e) receiver.

Offline DSP for transmitter	Offline DSP for receiver
PBRS	Down-converted
S/P	Schmidt orthogonalization
1024-IFFT	Resampling,CMA
Add CP	NNE
P/S	Hard-decision
Tenfold oversampling	Tenfold downsampling
DSM modulation	S/P,1024FFT,P/S, QAM demodulation
	BER calculation

Fig. 4. Offline DSP for transmitter and receiver.

To convert the signal generated from MATLAB from digital to analog, an arbitrary waveform generator (AWG, Tektronix AWG7122C) is employed. The W-band optical MMW signals are produced at the optical transmitter using two tunable external cavity lasers (ECL-1 and ECL-2) with linewidths of less than 100 kHz. Operating at a wavelength of 1550.67 nm, the ECL-2 serves as the optical local oscillator (LO) and exhibits a frequency offset of 88.5 GHz relative to ECL-1. Following the generation of a 10 Gbaud electrical signal from the AWG, the signal is amplified using a pair of parallel electrical amplifiers. By utilizing an I/Q modulator with a 3 dB bandwidth of 30 GHz, the continuous-wave (CW) lightwave emitted by ECL-1 is modulated with a 10 Gbaud electrical signal. The resulting modulated optical signal is then amplified using a polarization-maintaining erbium-doped fiber amplifier (PM-EDFA) and combined with the CW lightwave generated by ECL-2 using a polarization-maintaining optical coupler (PM-OC), based on optical heterodyne beating. An optical attenuator (ATT) is utilized to adjust the optical power of the signal before it is transmitted over 100 m of single-mode fiber (SMF). Subsequently, the signal is divided into two paths by an optical coupler (OC), with one path containing an optical delay line (DL) that provides a delay of 100 symbols, resulting in the elimination of the correlation between the two polarization-direction signals.

At W-band, two parallel photodiodes (PDs), each with a 3 dB bandwidth of 90 GHz, independently convert optical signals into electrical signals. The 88.5-GHz electrical signals are then sequentially passed through a W-band low noise amplifier (LNA) and a power amplifier (PA). The two wireless signals are combined using a horizontal/vertical (H/V) polarization multiplexer with a polarization isolation ratio exceeding 23 dB to produce a dual-polarized signal. This signal is then transmitted into free space using a conical antenna (CA) with a gain of 23 dBi. For long-range wireless transmission, two polytetrafluoroethylene (PTFE) lenses (Lens-1 and Lens-2) are utilized to collimate the radiation. After traversing a distance of 4.6 km, the dual-polarized wireless MMW signal is received by another PTFE lens (Lens-2) and the CA at the receiving end. The signal is then input into an H/V polarization demultiplexer and separated into two orthogonal polarization directions (H and V polarizations). These signals are first amplified by two parallel LNAs with a gain of 35 dB before being downconverted into intermediate frequency (IF) signals using a pair of mixers in the analog domain. Both mixers are driven by a 75 GHz radio-frequency local oscillator (RF LO) source, resulting in IF signals with carrier frequencies of approximately 13.5 GHz. Figure 5(a) displays the electrical spectrum of the received 13.5 GHz IF signal. The IF signals are further amplified by two identical electronic amplifiers (EAs) with a gain of 26 dB before being digitized and recorded by a real-time digital oscilloscope (OSC) via port-1 and port-3. The OSC used in this experiment (Tektronix, DSO73304D) has a sampling rate of 100 GSa/s and an electrical bandwidth of 33 GHz.

4. Results and Discussion

At the receiving end, the intermediate frequency signal is down-converted to obtain the baseband DSM signal. Then, the signal is subjected to Schmidt orthogonalization, resampling, CMA, and subsequent NNE to obtain the electrical spectrum of the signal, as shown in Fig. 5(b). The measured BER of DSM signal versus power into the PD at 88.5 GHz MMW frequencies in a 4.6 km wireless transmission is presented in Fig. 6, along with the

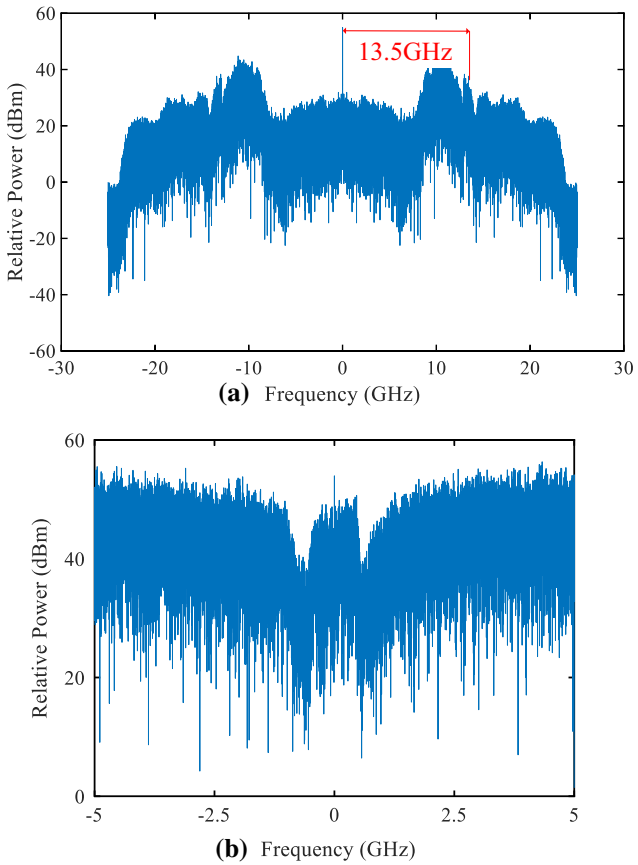

Fig. 5. (a) Electrical spectrum of received 13.5-GHz IF signals; (b) electrical spectrum of baseband signals after NNE.

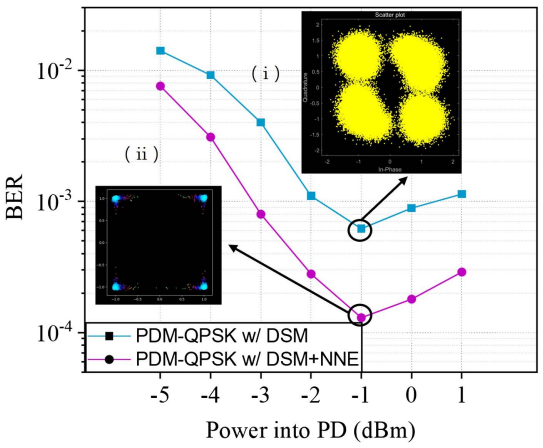

Fig. 6. Curves of BER versus power into the PD at the case of 10 Gbaud PDM-QPSK signal. (i) constellation with only DSM; (ii) constellation with DSM and NNE.

corresponding optimal constellations. Figure 6 shows that the system link has the optimal power into the PD, where an excessive amount leads to signal saturation and an insufficient amount leads to a low SNR. Long wireless transmission distances lead to a decrease in the SNR and an increase in nonlinearity due to wireless channel and optoelectronic device issues. Consequently, the BER of the inserted constellation (i) in Fig. 6 is not satisfactory when using solely DSM. Based on the implementation of DSM technology, NNE technology was further added to effectively improve the system's nonlinearity and obtain constellation (ii) in Fig. 6 with an ultralow BER. All subsequent experimental results integrated both DSM and NNE technologies. We perform hard decision on DSM signals with ultralow BERs, then perform 10 times downsampling on the DSM signal to achieve low-pass filtering of the DSM signal, and subsequently obtain the corresponding high-order QAM OFDM signal. Figure 7 shows the curves of BER versus power into the PD of 1 Gbaud high-order QAM signal. From the inserted constellation, we can see that as the order of the constellation increases, the constellation gradually blurs. However, the BER at 0.038 of 1 Gbaud 8192-QAM OFDM signal is still below the SD-FEC threshold of 0.04. The rate of PDM-8192-QAM OFDM signal is 23.4 Gbit/s [(2 × 980 × 13/((1024 + 64) × 10)) × 10 Gbaud].

In this Letter, many parameters are involved, including those related to devices and algorithms, as shown in the Tables 1–3 below.

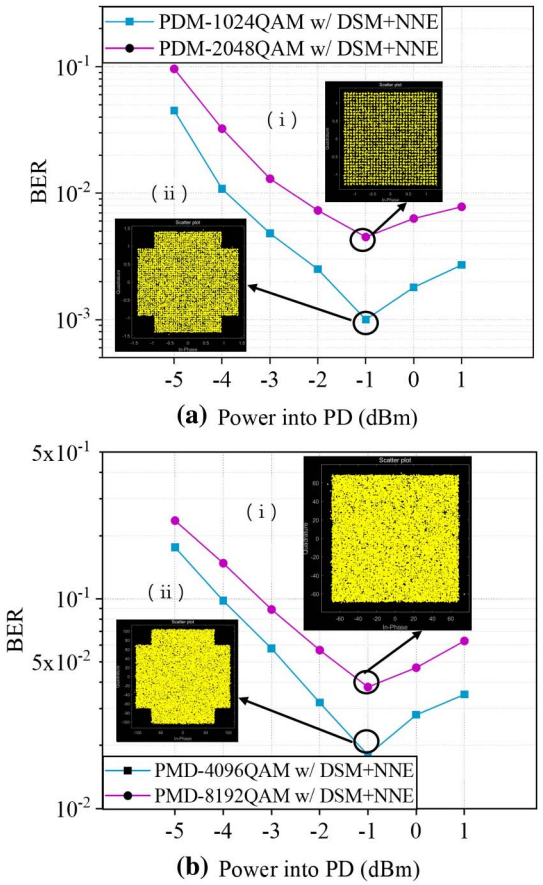

Fig. 7. Curves of BER versus power into the PD at the case of 1 Gbaud PDM-OFDM signal. (a) Constellation of 1024-QAM (i) and constellation of 2048-QAM (ii); (b) constellation of 4096-QAM (i) and constellation of 8192-QAM (ii).

Table 1. Parameters in the NNE.

Parameter	Value
Input size	62
Neural cells in hidden layer 1	40
Neural cells in hidden layer 2	20
Output size	2
Epoch	20
Optimizer	Adam
Batch size	64

Table 2. DSM Parameters.

Parameter	Value
OSR	10
Number of quantization bits	1
Synthesizing method	Chebyshev NTF
Order	6
Max NTF gain	1.55
NTF center frequency	0

Table 3. Important Devices Used in This Work.

Device	Model	Important Parameters
AWG	Tektronix AWG7122C	Sampling rate: 12 GSa/s
ECL	Agilent N7714A	Linewidth: <100 kHz
I/Q modulator	Fujitsu FTM7938EZ	3-dB bandwidth: 30 GHz
LNA	AT-LNA-75110	Gain: 21 dB
PA	AT-PA-80135-1320GN	Saturate output: 20 dBm
EA	CENTELLAX OA3MHQM	Gain: 25 dBm
PD	Finisar XPDV412xR	Bandwidth: 100 GHz
CA	SAC-2507-094-S2	Nominal gain: 25 dBi
OSC	Tektronix DSO73304D	Sampling rate: 100 GSa/s

5. Conclusion

This Letter presents an experimental demonstration of the wireless transmission of a PDM-8192-QAM signal over a distance of 4.6 km at 88.5 GHz in a W-band communication system. In order to further improve the performance of the system, NNE technology has been adopted. Compared to the scheme that uses only DSM, with the help of NNE technology, it can bring a sensitivity improvement of 1.2 dB when the FEC threshold is 1×10^{-3}. The successful transmission was achieved by applying DSM and NNE technologies, which utilized a 1-bit quantized DSM and nonlinear compensation of NNE to enable the long-distance transmission of high-order QAM signals in the W-band. This technology can be applied in future mobile fronthaul networks, which not only improves spectral efficiency, but also compensates for nonlinearity and reduces error rate. Otherwise, it can be used in cognitive radio systems to enhance spectrum sensing and dynamic spectrum access. It is worth noting that the DSP process in this paper is fully offline. When it comes to real-time implementation, the complexity and time delay must be taken into consideration. The complex digital filters in DSM and the multilayer structure of NNE both contribute a great deal of complexity and time delay. In the future work, we will focus on the complexity reduction of the proposed algorithms using techniques including pruning[22] and quantization[23], such as using sparse matrix multiplication or low-bitwidth arithmetic units, or implementing quantization-aware training methods.

Acknowledgements

This work was supported by the National Natural Science Foundation of China (Nos. 62225503, 61835005, and 62205151).

References

1. L. Zhao, B. Sang, Y. Tan, *et al.*, "Transmission of 1024-QAM OFDM at 28 GHz radio frequency using 5G millimeter wave phased array antenna," IEEE Trans. Microwave Theory Tech. **70**, 4211 (2022).
2. B. Skubic, M. Fiorani, S. Tombaz, *et al.*, "Optical transport solutions for 5G fixed wireless access [Invited]," J. Opt. Commun. Netw. **9**, D10 (2017).
3. Y.-W. Chen, R. Zhang, C.-W. Hsu, *et al.*, "Key enabling technologies for the post-5G era: fully adaptive, all-spectra coordinated radio access network with function decoupling," IEEE Commun. Mag. **58**, 60 (2020).
4. M. Huang, Y. Chen, P. Peng, *et al.*, "A full field-of-view self-steering beamformer for 5G mm-wave fiber-wireless mobile fronthaul," J. Light. Technol. **38**, 1221 (2020).
5. Z. Wang, Y. Xiao, S. Wang, *et al.*, "Security enhancement of W-band millimeter-wave based on 3-D Hilbert scrambling and diffusion," Opt. Express **29**, 17890 (2021).
6. X. Li, J. Yu, L. Zhao, *et al.*, "135-GHz D-band 60-Gbps PAM-8 wireless transmission employing a joint DNN equalizer with BP and CMMA," J. Lightwave Technol. **37**, 196 (2019).
7. L. Zhao, Y. Zhang, and W. Zhou, "Probabilistically shaped 64QAM OFDM signal transmission in a heterodyne coherent detection system," Opt. Commun. **434**, 175 (2019).
8. W. Zhou, L. Zhao, J. Zhang, *et al.*, "1-Tb/s millimeter-wave signal wireless delivery at D-band," J. Lightwave Technol. **37**, 196 (2020).
9. Y. Zhou, J. Xiao, L. Wang, *et al.*, "Simplified independent triple-sideband signal generation and transmission scheme based on one I/Q modulator at 0.3-THz," Opt. Express **31**, 9395 (2023).
10. Y. Zhou, J. Ming, L. Wang, *et al.*, "Optical polarization division multiplexing transmission system based on simplified twin-SSB modulation," Opt. Lett. **47**, 5317 (2022).
11. L. Zhao, K. Wang, and W. Zhou, "Transmission of 4096-QAM OFDM at D-band," Opt. Express **31**, 2270 (2023).
12. L. Zhao, S. Xu, M. Wang, *et al.*, "Probabilistic shaping-based delta sigma modulation," Opt. Lett. **48**, 1450 (2023).
13. J. Wang, Z. Yu, K. Ying, *et al.*, "Digital mobile fronthaul based on delta-sigma modulation for 32 LTE carrier aggregation and FBMC signals," J. Opt. Commun. Netw. **9**, A233 (2017).
14. L. Zhong, Y. Zou, S. Zhang, *et al.*, "An SNR-improved transmitter of delta-sigma modulation supported ultra-high-order QAM signal for Fronthaul/WiFi applications," J. Light. Technol. **40**, 2780 (2022).
15. F. Zhao, X. Yang, L. Zhao, *et al.*, "Demonstration of 4096QAM THz MIMO wireless delivery employing one-bit delta-sigma modulation," Opt. Lett. **47**, 6361 (2022).
16. K. Bai, D. Zou, Z. Zhang, *et al.*, "Digital mobile fronthaul based on performance enhanced multi-stage noise-shaping delta-sigma modulator," J. Light. Technol. **39**, 439 (2021).
17. J. Shi, B. Sang, W. Zhou, *et al.*, "65,536-QAM OFDM signal transmission over a fiber-THz system at 320 GHz with delta-sigma modulation," Opt. Lett. **48**, 602 (2023).
18. K. Wang, C. Wang, W. Li, *et al.*, "Complex-valued 2D-CNN equalization for OFDM signals in a photonics-aided MMW communication system at the D-band," J. Light. Technol. **40**, 2791 (2022).
19. I. Goodfellow, Y. Bengio, and A. Courville, *Deep Learning* (MIT Press, 2016).
20. C. C. Aggarwal, *Neural Networks and Deep Learning: A Textbook* (Springer, 2018).
21. W. Zhou, J. Shi, K. Wang, *et al.*, "Comparison of real- and complex-valued NN equalizers for photonics-aided 90-Gbps D-band PAM-4 coherent detection," J. Light. Technol. **39**, 6858 (2021).
22. B. Sang, W. Zhou, Y. Tan, *et al.*, "Low complexity neural network equalization based on multi-symbol output technique for 200+ Gbps IM/DD short reach optical system," J. Light. Technol. **40**, 2890 (2022).
23. A. Zhou, A. Yao, Y. Guo, *et al.*, "Incremental network quantization: towards lossless cnns with low-precision weights," arXiv:1702.03044 (2017).